Dyes and Pigments 134 (2016) 419–426

Contents lists available at ScienceDirect

Dyes and Pigments

journal homepage: www.elsevier.com/locate/dyepig

What difference does a thiophene make? Evaluation of a 4,4′-bis(thiophene) functionalised 2,2′-bipyridyl copper(I) complex in a dye-sensitized solar cell

Kathryn A. Wills [a], Humberto J. Mandujano-Ramírez [b, c], Gabriel Merino [b], Gerko Oskam [b], Paul Cowper [d], Matthew D. Jones [a, d, **], Petra J. Cameron [a, d, ***], Simon E. Lewis [a, d, *]

[a] Centre for Doctoral Training in Sustainable Chemical Technologies, University of Bath, Bath, BA2 7AY, UK
[b] Centro de Investigación y de Estudios Avanzados del IPN (Cinvestav), Departamento de Física Aplicada, Mérida, Yucatán, 97310, Mexico
[c] Facultad de Ingeniería, Universidad Autónoma del Carmen, Ciudad del Carmen, Campeche, 24115, Mexico
[d] Department of Chemistry, University of Bath, Bath, BA2 7AY, UK

ARTICLE INFO

Article history:
Received 11 June 2016
Received in revised form
14 July 2016
Accepted 16 July 2016
Available online 19 July 2016

Keywords:
Dye-sensitized solar cell
DSSC
Copper
Thiophene
Impedance spectroscopy

ABSTRACT

The synthesis of a 4,4′-bis(2-thienyl-5-carboxylic acid) functionalised 2,2′-bipyridine ligand and corresponding copper(I) complex is described and its application in a dye-sensitized solar cell (DSSC) is studied. The positioning of the thiophene groups appears favourable from DFT analysis and a best efficiency of 1.41% was obtained with this dye, for a 0.3 cm^2 cell area DSSC. Two absorbance bands are observed in the electronic absorption spectrum of the copper(I) complex at 316 nm and 506 nm, with ε values of 50,000 M^{-1} cm^{-1} and 9030 M^{-1} cm^{-1}, respectively. Cyclic voltammetry and electrochemical impedance spectroscopy are also used to provide a detailed analysis of the dye and assess its functionality in a DSSC.

1. Introduction

Over the past two decades, dye-sensitized solar cells (DSSCs) have established themselves as a promising and versatile technology for converting solar energy into electrical energy [1,2]. Improving the performance of the photosensitizing component in DSSCs has been extensively investigated, however the most stable are still generally ruthenium(II) complexes [3]. Organic dyes with the general form donor:π-bridge:acceptor (D-π-A) now rival metal-based complexes in terms of efficiency. Grätzel, Zakeeruddin, Yeh, Diau and co-workers reported a 12.3% efficiency cell, which was achieved by co-sensitizing a porphyrin dye and the organic dye Y123, in conjunction with a cobalt(II/III) electrolyte [4]. More recently, Grätzel et al. reported a 13% efficiency DSSC containing the SM315 dye [5]. Hanaya, Yano and co-workers reported a 12.8% efficiency DSSC using a dye with silyl anchoring groups [6]. Wang and co-workers reported a 12.5% efficiency DSSC using a dye containing an indenoperylene motif [7]. One issue with organic and porphyrin dyes is that they are usually the products of multi-step syntheses and purification can be challenging. There has also been a surge of interest in perovskite based solar cells in recent years, with efficiencies rapidly progressing beyond 20% [8]. However there is still a lot of work to be done on the stability of these cells and at present the understanding of their mechanism of action is incomplete.

Interest has grown in the replacement of ruthenium with a less expensive and more abundant metal, such as copper, to create complexes which have similar properties for DSSC application but without relying on scarce resources [9]. Copper(I) dyes have not yet been as extensively studied as their ruthenium(II) counterparts, although there have been a number of experimental and computational studies published in recent years. As early as 1983, Sauvage and co-workers were the first to demonstrate that a homoleptic bis(diimine) copper(I) complex could photosensitize a

* Corresponding author. Centre for Doctoral Training in Sustainable Chemical Technologies, University of Bath, Bath, BA2 7AY, UK.
** Corresponding author. Centre for Doctoral Training in Sustainable Chemical Technologies, University of Bath, Bath, BA2 7AY, UK.
*** Corresponding author. Centre for Doctoral Training in Sustainable Chemical Technologies, University of Bath, Bath, BA2 7AY, UK.
E-mail addresses: m.jones2@bath.ac.uk (M.D. Jones), p.j.cameron@bath.ac.uk (P.J. Cameron), s.e.lewis@bath.ac.uk (S.E. Lewis).

http://dx.doi.org/10.1016/j.dyepig.2016.07.023

semiconductor [10], and some years later Sakaki and co-workers disclosed the use in a DSSC of a homoleptic copper(I) complex comprising two bipyridyl ligands with 5,5'-carboxy groups [11]. These three publications constituted the entire literature on copper-based sensitizers in DSSCs, until a surge of interest in the area in the last eight years. Arguably, part of the increase in interest in copper DSSCs may be ascribed to a communication in 2008 from Constable, Housecroft and co-workers [12] (and the ensuing full paper [13]) which described the straightforward synthesis of a 6,6′-Dimethyl-2,2′-bipyridine-4,4′-dicarboxylic acid ligand **1** and the preparation of the corresponding analogous copper(I) complex [Cu(**1**)$_2$]Cl (Scheme 1). This complex was used to construct a DSSC having η = 1.9% (vs. η = 9.7% for an N719 cell prepared concurrently). A dye analogous to [Cu(**1**)$_2$]Cl with (*E*)-alkene spacers between the pyridine rings and carboxylic acid anchoring groups was also disclosed, and afforded a slightly higher efficiency (η = 2.3%).

Subsequent to the report of [Cu(**1**)$_2$]Cl, many further copper(I) dyes have been synthesised in the hope of improving cell efficiencies. To this end, many different design strategies have been pursued. A significant advance came with the reports of strategies to access heteroleptic copper(I) dyes, thus allowing for the synthesis of D-π-A type complexes. Whilst, ordinarily, heteroleptic copper(I) complexes are difficult to access in pure form due to ligand exchange establishing equilibria with the corresponding homoleptic complexes, two groups have demonstrated methods by which this problem can be overcome. Thus, the Constable/Housecroft group have developed a "Surfaces-as-ligands, surfaces-as-complexes" strategy [14], wherein a ligand bearing anchoring groups is first anchored onto the titania surface, then the surface is treated with a solution of a homoleptic complex of the other desired ligand; ligand metathesis occurs at the anchored ligand to give the desired heteroleptic complex on the surface. In contrast, Odobel et al. have successfully expanded on Schmittel's "HETPHEN" concept [15] to access heteroleptic complexes whereby one ligand is a 2,9-disubstituted-1,10-phenanthroline that is sufficiently sterically demanding that the unwanted homoleptic complex simply cannot form. Odobel et al. have used this approach to synthesise and evaluate numerous heteroleptic complexes [16], achieving a top efficiency of η = 4.66% (vs. η = 7.36% for an N719 cell prepared concurrently), when employing a bulky 6,6′-bis(mesityl)-2,2′-bipyridyl ligand with carboxylic acid anchoring groups, in conjunction with an electron-donating *p*-diethylaminostyryl bipyridine ancillary ligand [16c].

In addition to the above, other reports on copper(I) DSSCs have detailed the effects of different anchoring groups [14,17], of the introduction of halogen substituents [17i,m], of varying the electrolyte [17d,p,18], of dye bath concentration effects [17l], of introducing co-adsorbents [17h], and of incorporating hole-transport motifs [17e,g]. Robertson et al. have demonstrated the viability of DSSCs that employ copper(I) dyes containing a different class of bidentate ligand, namely a dipyrrin [19]. All of these reports, and others [20], provide a wealth of information on the effects, beneficial or otherwise, of these various design strategies. We ourselves previously investigated a homoleptic copper(I) dye with the 2,2′-biquinoline-4,4′-dicarboxylic acid (dcbiq) ligand but noted that efficiencies with this complex were low [21a]; other workers very recently suggested these low efficiencies were a consequence of a short excited-state lifetime due to exciplex formation [21b]. As an aside, it should also be noted that there have been reports of copper complexes being used in DSSCs not only as photosensitizers, but also as redox mediators [22].

The aim of the present study was to examine the effect of introducing a thiophene motif into the structure of a ligand for a Cu(I) dye, and evaluate a DSSC constructed with this dye, in comparison with one where the ligand lacked the thiophenes. There is significant precedent in the literature for the incorporation of thiophenes into the ligand framework of dyes for DSSCs. A recent review compared a number of ruthenium(II) dyes with thiophene moieties to the standard N3 or N719 dyes [23]. It was highlighted that all the complexes reviewed showed both a bathochromic and a

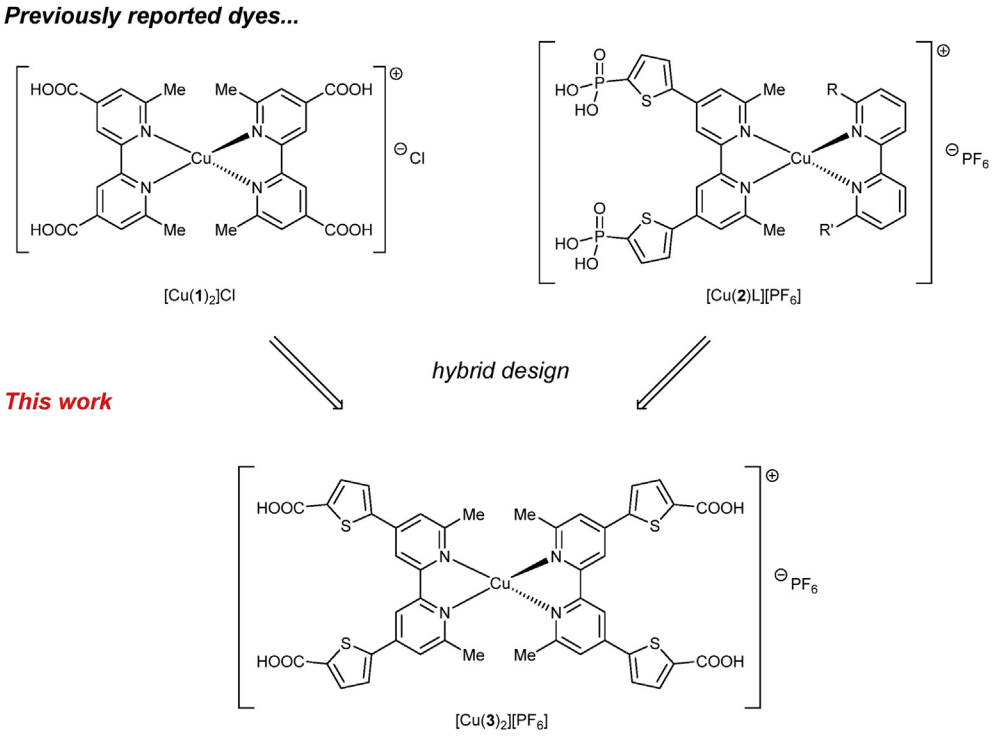

Scheme 1. Copper(I) dyes previously reported by Constable, Housecroft and co-workers and their influence on the design of the dye reported in this study.

hyperchromic shift in their absorption spectra relative to N3 or N719. The largest shift was for a ruthenium(II) complex, BTC-1, bearing two 4,4′-(5-carboxy-2-thienyl)-2,2′-bipy ligands, reported by Mishra, Zakeeruddin, Bäuerle, Grätzel and co-workers [24a]. In the BTC-1 dye, thiophene groups are incorporated *between* the bipyridine ligand and the anchoring carboxylic acid groups (as opposed to locating them on a non-binding ancillary ligand). It was found that this particular positioning of the ligand components lowered the LUMO energy of the sensitizers. Cells with a higher overall efficiency relative to N719 were achieved ($\eta = 6.1\%$ for BTC-1, vs. $\eta = 4.8\%$ for an N719 cell prepared concurrently). Elsewhere, a study of cyclometalated Ru(II) dyes sought to compare explicitly complexes bearing thiophene(s) on an ancillary ligand with those lacking such a motif [24b], finding that a dye comprising two thiophenes exhibited an efficiency more than twice that of the analogous dye without thiophenes.

This paper does not report the first example of a DSSC using a Cu(I) dye with thiophene-containing ligands; examples have already been published. In one report [17b], heteroleptic complexes including a single thiophene were evaluated; in contrast to the case of BTC-1, however, the thiophene was located on the ancillary ligand (i.e. not between the metal and the anchoring groups). In a more recent report [17o], heteroleptic complexes were reported comprising thiophenes in the anchoring ligand, between the bipyridyl motif and the anchoring groups (designated as [Cu(**2**)L]PF_6, depicted in Scheme 1). This same report also described complexes isomeric with [Cu(**2**)L]PF_6, with the anchoring group attached at the thiophene 4-position, which gave broadly similar efficiencies. For the purposes of assessing the specific effect of introducing the thiophene motif, we aimed to prepare a thiophene-containing Cu(I) dye to compare with an analogous dye lacking the thiophene motifs but equivalent in all other regards. Constable and Housecroft's archetypal homoleptic complex [Cu(**1**)$_2$]Cl was selected as the reference dye and so accordingly we targeted the thiophene-expanded [Cu(**3**)$_2$]PF_6 (Scheme 1). The synthesis of [Cu(**3**)$_2$]PF_6 and the construction and evaluation of DSSCs using this dye are reported in this paper. It should be noted that while the ligand **3** used here is similar to that used in the aforementioned ruthenium dye BTC-1, a crucial difference is that **3** incorporates methyl groups at the 6- and 6′-positions. These methyl groups impart essential steric bulk — as established previously in the literature [25,26] the design of copper(I) complexes needs to be carefully planned to prevent geometry changes upon oxidation from copper(I) to (II).

2. Results and discussion

2.1. Synthesis

As mentioned above, the target ligand **3** was very similar to that complexed to ruthenium by Mishra [24], however some steric bulk needed to be installed at the 6- and 6′-positions to retain geometric stability. For this reason, a synthesis was planned which had some similarity in its initial steps to that reported by Constable and co-workers for the 6,6′-dimethyl-2,2′-bipyridine-4,4′-dicarboxylic acid ligand **1** [12,13], but starting from 2-thiophenecarboxaldehyde **4** [27] rather than 2-furaldehyde (Scheme 2). The first step of the synthesis was modified slightly from the procedure used for the analogous 2-furaldehyde reaction. According to a report from Matsubara [28], 0.2 equivalents of acetic acid were included in addition to the other reagents, and the mixture was refluxed overnight. This offered an improved yield of **6** relative to the procedure previously followed, although still a relatively low one. Increasing the heating time did not result in any significant increase in yield.

The second step of the synthesis was a Kröhnke pyridine synthesis [29] to access compound **7**, which proceeded in the same way as with the analogous furan precursor, with a comparable (and moderate) yield. The next step was to derivatise the thiophene rings with the necessary anchoring moieties. In order to introduce carboxylic acid groups, bromination of the thiophene rings in the 5- and 5′- positions was first performed using elemental bromine to give **8**. No over-bromination was observed, although some optimisation of the bromine equivalents and reaction time had to be carried out in order to minimize the amount of mono-brominated product formed. A double lithium-halogen exchange on **8** was the next step, using *n*-BuLi and methyl chloroformate to install the methyl ester groups. The product, **9**, was isolated by column chromatography and hydrolysed under basic conditions to yield the final ligand, **3**. Of note, Constable, Housecroft and co-workers also reported the synthesis of **8** recently, but accessed it via a different synthetic route [17o]. Compounds **9** and **3** are previously unreported and have been fully characterised and assigned using 2D-NMR experiments. Crystals of **7** and **8** suitable for x-ray diffraction were obtained from slow evaporation of solvent (see ESI). Bipyridine **7** crystallised in the monoclinic crystal system with a $P2_1/n$ space group and adopts the same *trans*-conformation as the analogous bis(furan) compound [13]. The molecular structure is close to planar and the bond lengths and angles are similar for **7** and the analogous bis(furan) compound, with the exception of the expected differences in bond lengths between C-S and C-O. Bipyridine **8** also crystallised in the monoclinic crystal system, with a $C2/c$ space group. The *trans*-conformation, bond lengths and angles are analogous to those of **7** and the C-Br bond length is typical for a bromine atom attached to an aromatic carbon atom [30]. The packing of **8** in the unit cell shows that the molecules orient in layers, due to the π−π stacking between the aromatic rings. This arrangement is similarly reported for 6,6′-dimethyl-4,4′-di(2-furyl)-2,2′-bipyridine ligand [15]. The planarity and the *trans* configuration of both **7** and **8** follow from the fact that both structures are centrosymmetric.

Complexation of ligand **3** to copper was carried out under N_2 using [Cu(CH_3CN)$_4$]PF_6, dissolved in MeCN. A cannula transfer of the copper(I) precursor into a solution of **3** stirring at room temperature in basic MeOH (i.e. containing a quantity of aq. 1 M NaOH) was carried out. Formation of a clear, dark red, solution was immediate. This was stirred overnight under N_2 followed by reduction of the reaction mixture volume under vacuum and acidification to pH 4 with aq. 1 M HCl. A dark red solid precipitated, [Cu(**3**)$_2$]PF_6, and was isolated by filtration, washed with diethyl ether and dried. The analogous complexes [Cu(**7**)$_2$]PF_6 and [Cu(**9**)$_2$]PF_6 were also prepared in a similar manner. The presence of the $[PF_6]^-$ counter ion for the complexes was confirmed through $^{31}P\{^1H\}$ NMR. 2D-NMR data for [Cu(**9**)$_2$]PF_6 enabled complete proton and carbon assignment. An extended $^{13}C\{^1H\}$ acquisition detected 8 of the 9 aromatic carbons and the methyl carbon in compound [Cu(**3**)$_2$]PF_6. Whilst not all quaternary carbon environments were observed in the $^{13}C\{^1H\}$ NMR spectrum of [Cu(**3**)$_2$]PF_6, they could be identified via an HMBC experiment and by comparison with the data for [Cu(**9**)$_2$]PF_6, allowing a full assignment to be made.

2.2. UV/Vis spectroscopy

A UV/Vis spectrum was acquired for complex [Cu(**3**)$_2$]PF_6 both adsorbed on the TiO_2 surface and in solution. The spectrum of [Cu(**3**)$_2$]PF_6 adsorbed on the TiO_2 surface is broad but shows the same form as observed in solution (Fig. 1). The spectrum in solution exhibits an absorption maximum at $\lambda_{max} = 506$ nm, a molar extinction coefficient of $\varepsilon = 9030\ M^{-1}\ cm^{-1}$, which may be assigned to the metal-to-ligand charge transfer (MLCT) absorbance. There is also a very strong absorbance in the UV region, at λ_{max} 316 nm, with

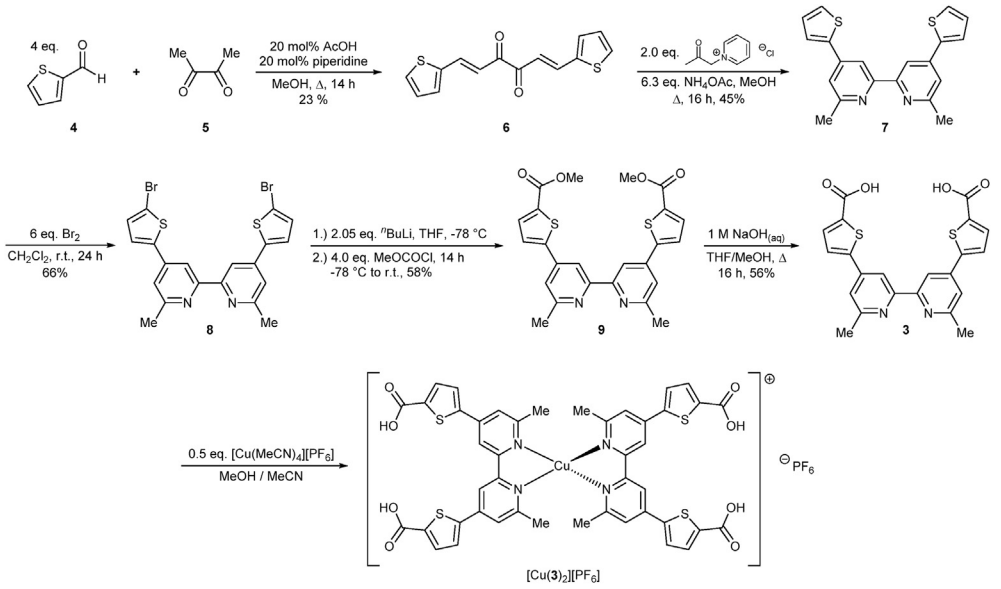

Scheme 2. Synthetic route to ligand **3** and complex $[Cu(\mathbf{3})_2]PF_6$.

$\varepsilon = 50{,}000\ M^{-1}\ cm^{-1}$, assigned to a $\pi \rightarrow \pi^*$ transition on the ligand. The analogous copper complex lacking the thiophene spacers, $[Cu(\mathbf{1})_2]Cl$, reportedly exhibits $\lambda_{max} = 483$ nm ($\varepsilon = 9900\ M^{-1}\ cm^{-1}$) and $\lambda_{max} = 319$ nm ($\varepsilon = 35{,}400\ M^{-1}\ cm^{-1}$) in the same solvent [13]. Thus, the expected bathochromic shift upon introduction of the thiophene motifs is clearly evident, with $\Delta\lambda_{max} = 23$ nm for the MLCT band. However, no appreciable hyperchromic shift (increase of ε) was observed for the MLCT band in $[Cu(\mathbf{3})_2]PF_6$ versus $[Cu(\mathbf{1})_2]Cl$; this is in contrast for the results reported for the ruthenium series of dyes [23].

2.3. Electrochemistry

Cyclic voltammograms were measured for $[Cu(\mathbf{3})_2]PF_6$ immobilised onto a TiO_2 film. The working electrode was a dyed TiO_2 film and undyed TiO_2 films were used for background scans. The counter electrode was a platinum wire and the reference electrode was Ag/AgCl (3 M KCl). CVs measured in a 0.2 M aqueous KNO_3 background electrolyte showed an oxidation process at low scan rates ($\leq$0.3 V/s), which became better defined as the scan rate was increased. At scan rates $\geq$0.5 V/s a reduction peak appeared which increased in magnitude with increasing scan rate. At the fastest scan rate recorded, 20 V/s, the CV looked close to reversible (Fig. 2). The peak oxidation and reduction potentials separated with increasing scan rate; at 1 V/s $E_p^{ox} = +0.56$ V and $E_p^{red} = +0.47$ V and at 20 V/s $E_p^{ox} = +0.65$ V and $E_p^{red} = +0.40$ V. Three TiO_2 films were measured and the same behaviour was seen in each measurement. The absence of a reduction peak at slow scan rates suggests that the oxidised species reacts/degrades chemically before it can be electrochemically reduced. Continuous cycling at 0.3 V s^{-1} led to a clear decrease in peak oxidation current over time. The cyclic voltammetry experiments were repeated in 0.1 M tetrabutylammonium hexafluorophosphate in MeCN, all other conditions were kept the same. In MeCN the same quasi-reversible CVs were observed, with an oxidation peak visible at slow scan rates and a reduction peak which appeared only at faster scan rates. Continuous scanning of a dyed film at 0.3 V s^{-1} under MeCN conditions found no drop in current over repeated cycling, implying that $[Cu(\mathbf{3})_2]PF_6$ is more stable on the TiO_2 surface in an MeCN environment.

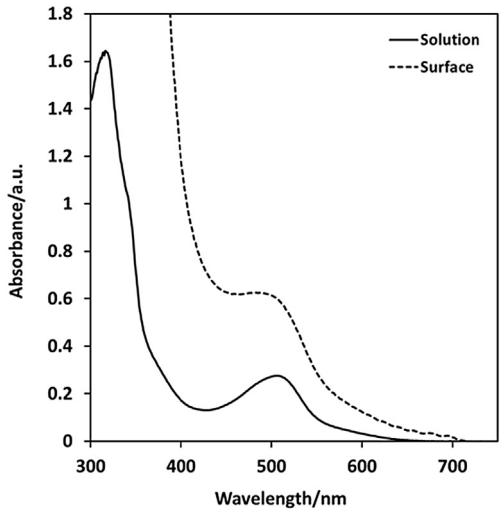

Fig. 1. UV/Vis spectrum of $[Cu(\mathbf{3})_2]PF_6$ in MeOH (32 μM) and adsorbed on a TiO_2 film.

2.4. Computational analysis

To understand further the electronic structure of $[Cu(\mathbf{3})_2]^+$, we carried out a series of computations using the M06 density functional approach in conjunction with the LANL2DZ basis set (Table 1). Solvent effects are taken into account to describe correctly the orbital splitting. The computed structure of $[Cu(\mathbf{3})_2]^+$ shows a slight deviation from C_2 symmetry with Cu-N bond lengths of 2.042 Å and N-Cu-N angles of 81.0°. The main contribution for the HOMO and HOMO−1 are the antibonding combination of the nitrogen lone pairs with the t_2 metal orbitals (64%, see Fig. 3). At lower energy ($\approx$1 eV with respect to the HOMO), there are three orbitals also with a predominant Cu-d character (ranging from 64 to 92%). LUMO and LUMO+1, almost degenerate, are antibonding orbitals resulting from combination of the carbon and nitrogen p

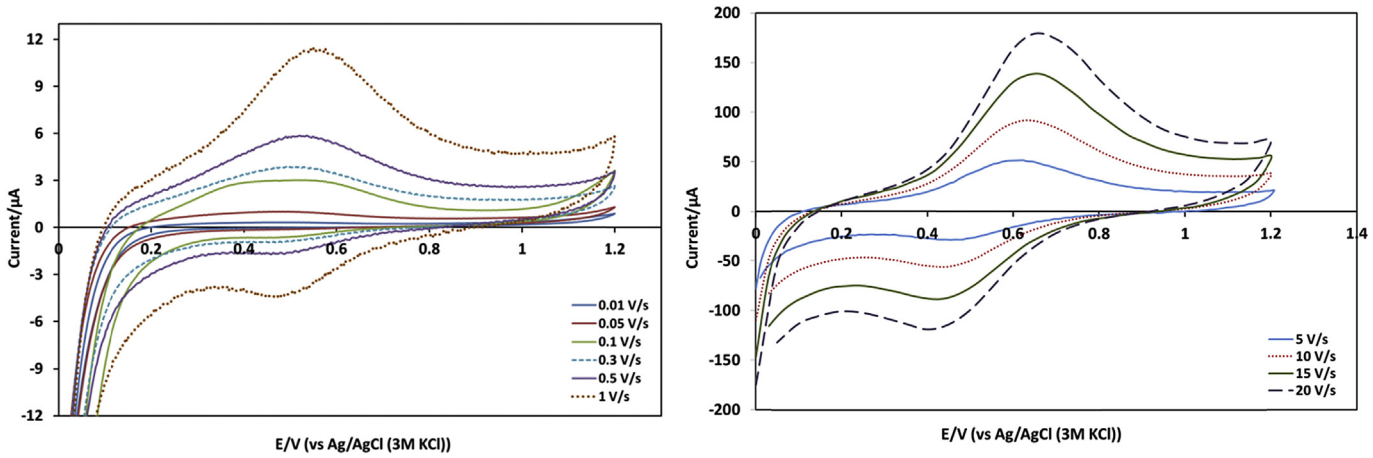

Fig. 2. Cyclic voltammograms of a dyed TiO_2 film with $[Cu(\mathbf{3})_2]PF_6$ at increasing scan rates (left graphic shows 10 mV to 1 V s^{-1}, right graphic shows 5 V–20 V s^{-1}). The supporting electrolyte is 0.2 M aqueous KNO_3, Ag/AgCl reference electrode and a Pt counter electrode.

atomic orbitals and have a significant contribution from the thiophene ring and the carboxylic acid functional group.

The carboxylic acid groups act as anchors to the TiO_2 semiconductor surface, favouring the electron injection from the dye excited state into the semiconductor conduction band. The computed HOMO energy (−5.80 eV) is close to those of N3 (−5.6 eV) and N719 (−5.5 eV) [31]. The estimated HOMO–LUMO gap is 3.06 eV. The excitation energies and oscillator strengths for the most important optical transitions are reported in Table 2, together with the composition of the solution vectors in terms of the most relevant transitions. Multiple MLCT transitions occur at 555 nm, mainly excitations from HOMO and HOMO−1, which correspond to one-electron excitations from t_2-π^*/t_2-π to π^* ligand levels. The value computed is somewhat far from the experimental data (506 nm). Our computations reproduce the experimental band at 316 nm quite well. This absorption band involves transitions from HOMO−9 and HOMO−8 to LUMO. The complex lacking the thiophenes, $[Cu(\mathbf{1})_2]PF_6$, has been modelled computationally; our calculated HOMO energy for $[Cu(\mathbf{3})_2]PF_6$ of −5.80 eV is higher than the reported calculated value for $[Cu(\mathbf{1})_2]PF_6$ of −6.16 eV [32]. The tetrakis (methyl ester) analogue of $[Cu(\mathbf{1})_2]PF_6$ has also been modelled computationally [33], albeit with a different functional and basis set.

2.5. Behaviour of the dye in DSSCs

DSSCs were manufactured using $[Cu(\mathbf{3})_2]PF_6$. Initially cells were made with a 1 cm^2 active area and either a single or double layer of TiO_2 (≈7 μm or 14 μm) Two electrolyte compositions were used, which varied in their volatility and in the quantities of iodine and iodide (see ESI for full details). All cells were unmasked. Promising efficiencies of between 0.61 and 0.74% were obtained with a 1 cm^2 active area. Cell parameters measured for DSSCs with $[Cu(\mathbf{3})_2]PF_6$, compared to cells containing N719 dye, are given in the ESI. All the device efficiencies were low (in particular for the N719 cells), but the results were obtained for non-optimised devices with a 1 cm^2 active area. The experiment found that cells with thinner TiO_2 films displayed a modest improvement in short-circuit photocurrent, open-circuit photovoltage and overall solar-to-electrical power conversion efficiency compared to those assembled from thicker TiO_2 films.

Optimisation of DSSCs with $[Cu(\mathbf{3})_2]PF_6$ was then carried out. The cell area was reduced, a TiO_2 scattering layer was applied and a post-sintering $TiCl_4$ treatment was carried out. By employing these additional treatments, a single layer TiO_2 cell with electrolyte 2 resulted in a top DSSC efficiency with $[Cu(\mathbf{3})_2]PF_6$ of 1.41%, measured at 1 sun. In this set of experiments improvements were observed if the DSSCs were left to "rest" overnight after assembly. The short circuit current increased between day 0 and day 1 leading to an increase in efficiency (see cells 1–3, Table 3, Fig. 4). This ageing effect of copper(I) DSSCs has also been observed by other groups [2,16a,20a]. The reason for this effect is poorly understood, however it is suggested that reorganization, or aggregation, of dye molecules on the TiO_2 surface may be responsible [16a,20a]. The top DSSC efficiency of $\eta = 1.41\%$ for $[Cu(\mathbf{3})_2]PF_6$ must be considered in the context of the top observed efficiency of $\eta = 3.12\%$ for the N719 cells prepared concurrently. Comparing these two efficiencies gives $\eta/\eta_{N719} = 45.2\%$. On the other hand, whereas the headline efficiency reported for comparator dye $[Cu(\mathbf{1})_2]Cl$ was $\eta = 1.9\%$, this should also be considered in the context of the observed efficiency of $\eta = 9.7\%$ for an N719 cell prepared concurrently [12]. In this latter case, therefore, $\eta/\eta_{N719} = 20\%$. As such, our results suggest that significant gains in relative cell efficiency can be achieved solely through the introduction of thiophene motifs into the ligand backbone.

The $[Cu(\mathbf{3})_2]PF_6$ cells were retested after 6 weeks in the dark (see ESI). Cells 1 and 3 still retained a very respectable performance with efficiencies of 1.21 and 0.89% respectively. (Cell 2 leaked leading to a drop in efficiency to 0.21%). All cells showed a small increase in V_{OC} of between 10 and 16 mV after being stored. The main change was in the J_{SC}, which could be due to dye desorption from TiO_2 or a degradation of the dye due to the electrolyte or presence of water over time [34,35]. However, with good cell sealing, $[Cu(\mathbf{3})_2]PF_6$ appears stable in a DSSC environment at least for several weeks

Table 1
Summary of detailed analysis of relevant frontier orbitals for $[Cu(\mathbf{3})_2]^+$.

MO	*E* (eV)	Cu (% contribution)
LUMO+1	−2.72	0
LUMO	−2.74	0
HOMO	−5.80	64 (d_{xy})
HOMO−1	−5.82	64 (d_{xz})
HOMO−2	−6.73	84 (d_{yz})
HOMO−3	−6.80	64 (d_{z^2})
HOMO−4	−7.02	92 (d^{22}_{x-y})

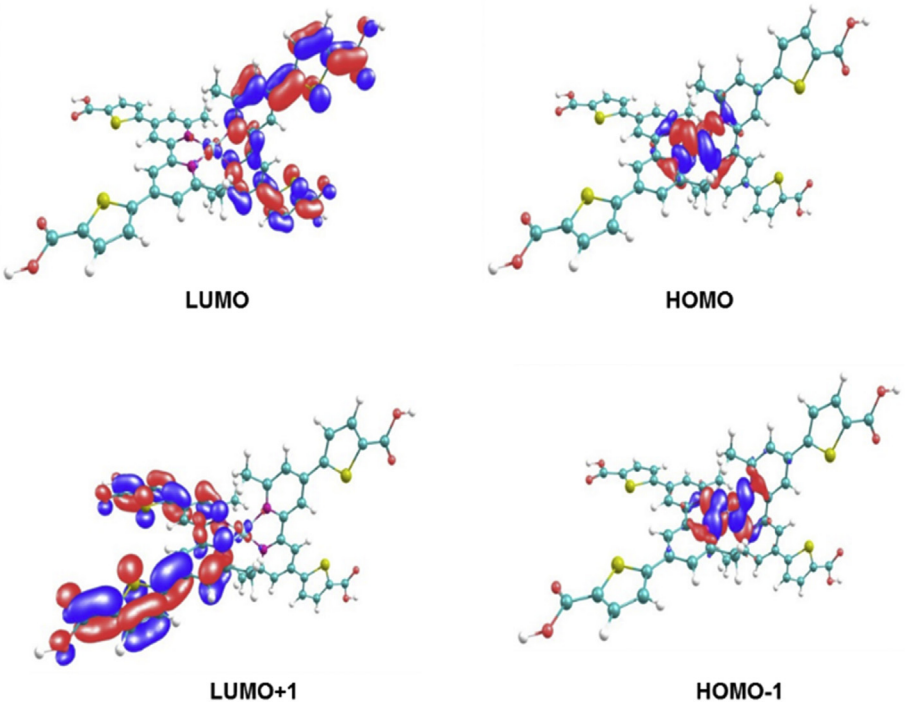

Fig. 3. The relevant frontier orbitals of $[Cu(\mathbf{3})_2]^+$.

Table 2
Wavelength, oscillator strength and composition of the most important optical transitions.

Energy (nm)	f	Composition
555.66	0.55	HOMO−1 → LUMO (22%), HOMO−1 → LUMO+1 (24%) HOMO → LUMO (26%), HOMO → LUMO+1 (20%)
347.12	0.69	HOMO−3 → LUMO+2 (63%), HOMO−3 → L+3 (29%)
338.56	0.36	HOMO−7 → LUMO (82%)
337.16	0.30	HOMO−6 → LUMO+1 (73%)
327.55	0.10	HOMO-5 → LUMO (25%), HOMO−5 → LUMO+1 (25%)
327.51	0.11	HOMO−5 → LUMO (22%), HOMO−5 → LUMO+1 (29%)
319.09	1.43	HOMO−9 → LUMO (42%), HOMO−8 → LUMO (13%), HOMO−8 → LUMO+1 (15%)

with very reasonable solar-to-power conversion efficiencies possible.

2.6. IPCE and electrochemical impedance spectroscopy

The incident photon to current efficiency (IPCE) spectrum for an unoptimised 1 cm^2 DSSC with $[Cu(\mathbf{3})_2]PF_6$ is shown in Fig. 5, and compared to that of an N719 cell. Both cells were prepared with a double layer of TiO_2 paste (film thickness ≈14 μm) and there was no scattering layer or $TiCl_4$ treatment used. It can be seen that there is a broad spectral response from ≈600 nm with $[Cu(\mathbf{3})_2]PF_6$ and the peak visible-region maxima was 17% at 500 nm. Spectra recorded for other unoptimised DSSCs with $[Cu(\mathbf{3})_2]PF_6$, including ones with a single TiO_2 layer, showed the same shape and the maximum IPCE was always between 14% and 17%.

A low IPCE (external quantum efficiency) can be due to poor light absorption, electron injection efficiency, low charge collection efficiency, or a combination of these factors. Charge collection efficiency can be reduced if there is a high degree of recombination of injected electrons with the oxidised redox mediator. The

Table 3
Comparing cell parameters on day 0/*day 1*day 1 for DSSCs with a single layer of TiO_2 and a scattering layer (particle size 150–250 nm) with $TiCl_4$. [a]N719 cell efficiency on day 0 used for calculation of η/ηN719.

Dye	Cell ID	Cell area (cm^2)	V_{OC} (mV)	J_{SC} (mA)	*FF* (%)	η (%)	η/η_{N719}[a] (%)
$[Cu(\mathbf{3})_2]PF_6$	Cell 1	0.30	552/ *563*	2.95/ *3.60*	71.3/ *69.8*	1.16/ *1.41*	37.1/ *45.2*
$[Cu(\mathbf{3})_2]PF_6$	Cell 2	0.25	579/ *593*	2.88/ *3.30*	62.6/ *59.9*	1.04/ *1.17*	33.3/ *37.5*
$[Cu(\mathbf{3})_2]PF_6$	Cell 3	0.275	560/ *575*	3.01/ *3.57*	62.9/ *54.6*	1.06/ *1.12*	34.0/ *35.9*
N719	-	0.30	657/ *670*	9.42/ *9.24*	50.5/ *40.9*	3.12/ *2.53*	*n/a*

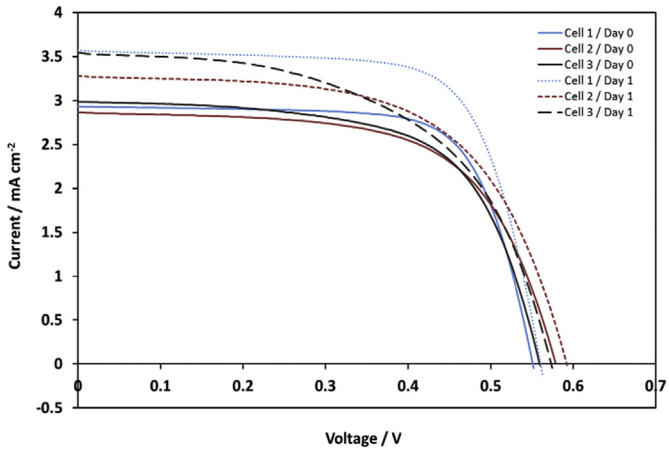

Fig. 4. I-V curves, recorded at 1 sun on day 0 and day 1, of cells assembled with $[Cu(\mathbf{3})_2]PF_6$. Cell parameters are given in Table 3.

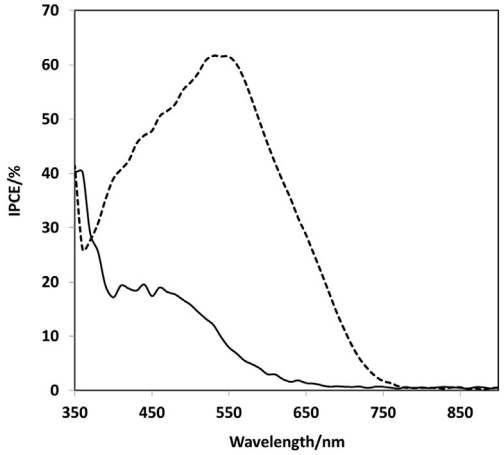

Fig. 5. IPCE spectra for DSSCs with $[Cu(\mathbf{3})_2]PF_6$ (solid line) and N719 (dashed line) compared.

electron diffusion length is a measurable indicator of this and was probed using electrochemical impedance spectroscopy. Measurements under two different light intensities (photon fluxes of 2.66×10^{15} and 3.64×10^{15} s^{-1} cm^{-2}) were recorded at open-circuit potential and EIS data for the two DSSCs studied are tabulated in Table 4. For the N719 DSSC, the DX type 11-Bisquert #2 equivalent circuit model [36] was used, although the Warburg element was omitted since no Warburg impedance was observed in the experiment. For an efficient DSSC it is necessary that the recombination resistance for electrons in the TiO_2 film is greater than the transport resistance ($r_{rec} > r_{tr}$). Using these values the electron diffusion length (L_n) and effective electron lifetime (τ_n) were calculated. It can be seen that for the control N719 DSSC, L_n is greater than the TiO_2 film thickness, L, as is required to prevent recombination limiting the performance of the DSSC. There is negligible variation in L_n with change in light intensity, which concurs with discussion in the literature [37]. DSSCs with $[Cu(\mathbf{3})_2][PF_6]$ exhibited slightly different impedance responses than observed with N719. Fitting of the data was initially attempted with the DX type 11-Bisquert #2 model. However since the counter electrode impedance was not clearly visible, the R1 and C1 elements were removed, resulting in a modified equivalent circuit model. Details of the equivalent circuits used can be found in the supplementary information. It is noted that comparisons between the N719 and $[Cu(\mathbf{3})_2][PF_6]$ EIS measurements can only be made for the electron diffusion length. Different dyes can change the density of states distribution in the TiO_2 film and as a result there is no guarantee that the charge density is the same at the same measured voltage. As a result, electron lifetimes cannot be directly compared, however the electron diffusion length, L_n, can be compared. In the present study, all electron diffusion lengths are adequate relative to the TiO_2 film thickness.

3. Conclusions

The complex $[Cu(\mathbf{3})_2]PF_6$ has been synthesised, studied and screened in a DSSC. The data obtained have been compared with those reported for the analogous dye lacking thiophene motifs, $[Cu(\mathbf{1})_2]Cl$. Respectable DSSC performances for a copper(I) dye have been obtained for $[Cu(\mathbf{3})_2]PF_6$, with a top efficiency of $\eta = 1.41\%$ ($\eta/\eta_{N719} = 45.2\%$). The complex exhibited two absorbance bands in the electronic absorption spectrum at 316 nm and 506 nm, with ε values of 50,000 M^{-1} cm^{-1} and 9030 M^{-1} cm^{-1}, respectively. DFT computations indicate that multiple MLCT transitions occur at 555 nm, mainly excitations from HOMO and HOMO−1, which correspond to one-electron excitations from t_2-π^*/t_2-π to π^* ligand levels. The two electrolyte compositions used, which differed in the volatility of their components, did not particularly affect the DSSC performance. However cells with thinner TiO_2 films (6–7 μm) displayed a modest improvement in short-circuit current, open-circuit photovoltage and overall solar-to-electrical power conversion efficiency compared to those assembled from thicker TiO_2 films (14–15 μm). A "ripening" effect in the cells was noted when comparing I-V measurements from the day of construction to measurements made the following day. Cyclic voltammetry showed that the dye underwent redox cycling, attributed to the Cu(I)/Cu(II) transitions, in both aqueous and MeCN background electrolyte solutions. An oxidation reaction was always observed, however the reduction was found to be scan rate dependent. The electron diffusion length for $[Cu(\mathbf{3})_2]PF_6$ was greater than the TiO_2 film thickness, as required. It can be concluded that the required electron kinetic processes are taking place reasonably effectively, as evidenced by the aforementioned respectable solar-to-power-conversion efficiencies recorded (for a copper(I) dye). Regarding comparisons between $[Cu(\mathbf{3})_2]PF_6$ and $[Cu(\mathbf{1})_2]Cl$, a bathochromic shift of the MLCT absorbance, a raising of the computed HOMO energy level and a higher η/η_{N719} value have all been noted. Our results argue for the more widespread incorporation of thiophene motifs in ligands for copper(I) complexes for use in DSSCs.

Table 4
EIS data for N719 and $[Cu(\mathbf{3})_2][PF_6]$ compared.

Dye	Photon flux (s^{-1} cm^{-2})	Film thickness	V_{oc}	R2 (Ω)	r_{tr} (Ω)	r_{rec} (Ω)	c_μ (mF)	L_n (μm)	τ_n (ms)
N719	2.66×10^{15}	13.2 μm	0.680	12.56	3.48	15.38	1.58	27.7	24.3
	3.64×10^{15}		0.682	12.47	2.71	11.51	1.90	27.2	21.9
$[Cu(\mathbf{3})_2][PF_6]$	2.66×10^{15}	15.4 μm	0.527	8.77	20.6	69.4	0.13	28.2	9.03
	3.64×10^{15}		0.537	9.34	19.0	51.0	0.16	25.2	8.11

Acknowledgements

We thank the EPSRC for funding (CDT PhD studentship for Kathryn Wills, Grant EP/G03768X/1). We acknowledge the General Coordination of Information and Communications Technologies (CGSTIC) at CINVESTAV for providing HPC resources on the Hybrid Cluster Supercomputer "Xiuhcoatl". The work in Mérida was supported by Conacyt (grants CB-2012-178510 and CB-2015-252356).

Appendix A. Supplementary data

Supplementary data related to this article can be found at http://dx.doi.org/10.1016/j.dyepig.2016.07.023.

References

[1] O'Regan B, Grätzel M. Nature 1991;353:737–40.
[2] Desilvestro J, Grätzel M, Kavan L, Moser J, Augustynski J. J Am Chem Soc 1985;107:2988–90.
[3] Nazeeruddin MK, Baranoff E, Grätzel M. Sol Energy 2011;85:1172–8.
[4] Yella A, Lee H-W, Tsao HN, Yi C, Chandiran AK, Nazeeruddin MK, et al. Science 2011;334:629–34.
[5] Mathew S, Yella A, Gao P, Humphry-Baker R, Curchod BFE, Ashari-Astani N, et al. Nat Chem 2014;6:242–7.
[6] Kakiage K, Aoyama Y, Yano T, Oya K, Kyomen T, Hanaya M. Chem Commun 2015;51:6315–7.
[7] Yao Z, Zhang M, Wu H, Yang L, Li R, Wang P. J Am Chem Soc 2015;137:3799–802.
[8] (a) Stranks SD, Snaith HJ. Nat Nanotechnol 2015;10:391.
(b) Kazim S, Nazeeruddin MK, Grätzel M, Ahmad S. Angew Chem Int Ed 2014;53:2812–24.
(c) Green MA, Ho-Baillie A, Snaith HJ. Nat Photonics 2014;8:506–14.
[9] For reviews, see: (a) Sandroni M, Pellegrin Y, Odobel F. C R Chim 2016;19:79–93.
(b) Housecroft CE, Constable EC. Chem Soc Rev 2015;44:8386–98.
(c) Mara MW, Fransted KA, Chen LX. Coord Chem Rev 2015;282–283:2–18.
(d) Lazorski MS, Castellano FN. Polyhedron 2014;82:57–70.
(e) Bozic-Weber B, Constable EC, Housecroft CE. Coord Chem Rev 2013;257:3089–106.
(f) Rendondo AH, Constable EC, Housecroft CE. Chimia 2009;63:205–7.
(g) Robertson N. ChemSusChem 2008;1:977–9.
[10] (a) Vante NA, Ern V, Chartier P, Dietrich-Buchecker CO, McMillin DR, Marnot PA, et al. Nouv J Chim 1983;7:3–5.
(b) Alonso-Vante N, Nierengarten J-F, Sauvage J-P. Dalton Trans 1994:1649–54.
[11] Sakaki S, Kuroki T, Hamada T. Dalton Trans 2002:840–2.
[12] Bessho T, Constable EC, Grätzel M, Redondo AH, Housecroft CE, Kylberg W, et al. Chem Commun 2008:3717–9.
[13] Constable EC, Redondo AH, Housecroft CE, Neuburger M, Schaffner S. Dalton Trans 2009:6634–44.
[14] Schönhofer E, Bozic-Weber B, Martin CJ, Constable EC, Housecroft CE, Zampese JA. Dyes Pigments 2015;115:154–65.
[15] (a) Schmittel M, Ganz A, Fenske D, Herderich M. Dalton Trans 2000:353–9.
(b) Schmittel M, Luning U, Meder M, Ganz A, Michel C, Herderich M. Heter Commun 1997;3:493–8.
(c) Schmittel M, Ganz A. Chem Commun 1997:999–1000.
[16] (a) Sandroni M, Kayanuma M, Planchat A, Szuwarski N, Blart E, Pellegrin Y, et al. Dalton Trans 2013;42:10818–27.
(b) Sandroni M, Kayanum M, Rebarz M, Akdas-Kilig H, Pellegrin Y, Blart E, Le Bozec H, et al. Dalton Trans 2013;42:14628–38.
(c) Sandroni M, Favereau L, Planchat A, Akdas-Kilig H, Szuwarski N, Pellegrin Y, et al. J Mater Chem A 2014;2:9944–7.
[17] (a) Constable EC, Housecroft CE, Neuburger M, Price J, Wolf A, Zampese JA. Inorg Chem Commun 2010;13:74–6.
(b) Bozic-Weber B, Constable EC, Housecroft CE, Kopecky P, Neuburger M, Zampese JA. Dalton Trans 2011;40:12584–94.
(c) Bozic-Weber B, Chaurin V, Constable EC, Housecroft CE, Meuwly M, Neuburger M, et al. Dalton Trans 2012;41:14157–69.
(d) Bozic-Weber B, Constable EC, Furer SO, Housecroft CE, Troxler LJ, Zampese JA. Chem Commun 2013;49:7222–4.
(e) Bozic-Weber B, Brauchli SY, Constable EC, Fuerer SO, Housecroft CE, Wright IA. Phys Chem Chem Phys 2013;15:4500–4.
(f) Bozic-Weber B, Brauchli SY, Constable EC, Furer SO, Housecroft CE, Malzner FJ, et al. Dalton Trans 2013;42:12293–308.
(g) Brauchli SY, Bozic-Weber B, Constable EC, Hostettler N, Housecroft CE, Zampese JA. RSC Adv 2014;4:34801–15.
(h) Brauchli SY, Malzner FJ, Constable EC, Housecroft CE. RSC Adv 2014;4:62728–36.
(i) Malzner FJ, Brauchli SY, Constable EC, Housecroft CE, Neuburger M. RSC Adv 2014;4:48712–23.
(j) Malzner FJ, Brauchli SY, Schönhofer E, Constable EC, Housecroft CE. Polyhedron 2014;82:116–21.
(k) Brauchli SY, Malzner FJ, Constable EC, Housecroft CE. RSC Adv 2015;5:48516–25.
(l) Brauchli SY, Constable EC, Housecroft CE. Dyes Pigments 2015;115:447–50.
(m) Brunner F, Klein YM, Keller S, Morris CD, Prescimone A, Constable EC, et al. RSC Adv 2015;5:58694–703.
(n) Fürer SO, Bozic-Weber B, Neuburger M, Constable EC, Housecroft CE. RSC Adv 2015;5:69430–40.
(o) Klein YM, Willgert M, Prescimone A, Constable EC, Housecroft CE. Dalton Trans 2016;45:4659–72.
(p) Fürer SO, Luu LYN, Bozic-Weber B, Constable EC, Housecroft CE. Dyes Pigments 2016;132:72–8.
(q) Büttner A, Brauchli SY, Vogt R, Constable EC, Housecroft CE. RSC Adv 2016;6:5205.
[18] (a) Ashbrook LN, Elliott CM. J Phys Chem C 2013;117:3853–64.
(b) Colombo A, Dragonetti C, Magni M, Roberto D, Demartin F, Caramori S, et al. ACS Appl Mater Interfaces 2014;6:13945–55.
[19] Hewat TE, Yellowlees LJ, Robertson N. Dalton Trans 2014;43:4127–36.
[20] (a) Bozic-Weber B, Constable EC, Housecroft CE, Neuburger M, Price JR. Dalton Trans 2010;39:3585–94.
(b) Linfoot CL, Richardson P, Hewat TE, Moudam O, Forde MM, Collins A, et al. Dalton Trans 2010;39:8945–56.
(c) Lu XQ, Wei SX, Wu CML, Li SR, Guo WY. J Phys Chem C 2011;115:3753–61.
(d) Yuan Y-J, Yu Z-T, Zhang J-Y, Zou Z-G. Dalton Trans 2012;41:9594–7.
(e) Huang J, Buyukcakir O, Mara MW, Coskun A, Dimitrijevic NM, Barin G, et al. Angew Chem Int Ed 2012;51:12711–5.
(f) Colombo A, Dragonetti C, Roberto D, Valore A, Biagini P, Melchiorre F. Inorg Chim Acta 2013;407:204–9.
(g) Martin CJ, Bozic-Weber B, Constable EC, Glatzel T, Housecroft CE, Wright IA. J Phys Chem C 2014;118:16912–8.
(h) Magnia M, Colombo A, Dragonetti C, Mussini P. Electrochim Acta 2014;141:324–30.
(i) Martin CJ, Bozic-Weber B, Constable EC, Glatzel T, Housecroft CE, Wright IA. Electrochim Acta 2014;119:86–91.
(j) Huang T-H, Yan J, Yang H, Du H-M, Zhang M-H. J Coord Chem 2015;68:1514–27.
(k) Huang T-H, Yan J, Liu Y-F, Xie Y-T, Jia C. Aust J Chem 2015;68:1144–51.
(l) Mara MW, Bowman DN, Buyukcakir O, Shelby ML, Haldrup K, Huang J, et al. J Am Chem Soc 2015;137:9670–84.
(m) Wei S, Shao Y, Shi X, Lu X, Li K, Zhao Z, et al. Org Electron 2016;29:142–50.
[21] (a) Wills KA, Mandujano-Ramirez HJ, Merino G, Mattia D, Hewat T, Robertson N, et al. RSC Adv 2013;3:23361–9.
(b) Fransted KA, Jackson NE, Zong R, Mara MW, Huang J, Harpham MR, et al. J Phys Chem A 2014;118:10497–506.
[22] (a) Magni M, Biagini P, Colombo A, Dragonetti C, Roberto D, Valore A. Coord Chem Rev 2016;322:69–93.
(b) Freitag M, Giordano F, Yang W, Pazoki M, Hao Y, Zietz B, et al. J Phys Chem C 2016;120:9595–603.
(c) Magni M, Giannuzzi R, Colombo A, Cipolla MP, Dragonetti C, Caramori S, et al. Inorg Chem 2016;55:5245–53.
(d) Hattori S, Wada Y, Yanagida S, Fukuzumi S. J Am Chem Soc 2005;127:9648–54.
[23] Abbotto A, Manfredi N. Dalton Trans 2011;40:12421–38.
[24] (a) Mishra A, Pootrakulchote N, Fischer MKR, Klein C, Nazeeruddin MK, Zakeeruddin SM, et al. Chem Commun 2009:7146–8.
(b) Abbotto A, Coluccini C, Dell'Orto E, Manfredi N, Trifiletti V, Salamone MM, et al. Dalton Trans 2012;41:11731–8.
[25] Gil B, Draper SM. In: Pignataro B, editor. Ideas in chemistry and molecular sciences: advances in nanotechnology, materials and devices. Weinheim, Germany: Wiley-VCH; 2010. p. 339–56.
[26] Williams RM, De Cola L, Hartl F, Lagref JJ, Planeix JM, De Cian A, et al. Coord Chem Rev 2002;230:253–61.
[27] Sun Y-F, Zhong L, Hou X-M, Ma S-Y, Duan W-Z, Wu R-T. Color Technol 2012;128:331–9.
[28] Takada Y, Nomura K, Matsubara S. Org Lett 2010;12:5204–5.
[29] Kröhnke F. Synthesis 1976:1–24.
[30] James MNG, Williams GJB. Acta Crystallogr B 1973;29:1172–4.
[31] Nazeeruddin MK, De Angelis F, Fantacci S, Selloni A, Viscardi G, Liska P, et al. J Am Chem Soc 2005;127:16835–47.
[32] Baldenebro-Lopez J, Flores-Holguin N, Castorena-Gonzalez J, Almaral-Sanchez J, Glossman-Mitnik D. Int J Photoenergy 2013:613064.
[33] Lu X, Wu C-ML, Wei S, Guo W. J Phys Chem A 2010;114:1178–84.
[34] Heo N, Jun Y, Park JH. Sci Rep 2013;3:1712.
[35] Macht B, Turrion M, Barkschat A, Salvador P, Ellmer K, Tributsch H. Sol Energy Mater Sol Cells 2002;73:163–73.
[36] Bisquert J, Fabregat-Santiago F. In: Kalyanasundaram K, editor. Dye-sensitized solar cells. EPFL Press; 2010. p. 457–554.
[37] Peter LM, Wijayantha KGU. Electrochim Acta 2000;45:4543–51.